ARL-TR-9879 ● FEB 2024

Resolution as a Computational Factor in CTH Simulations of a Shaped-Charge Jet

by Daniel J Hornbaker

NOTICES

Disclaimers

The findings in this report are not to be construed as an official Department of the Army position unless so designated by other authorized documents.

Citation of manufacturer's or trade names does not constitute an official endorsement or approval of the use thereof.

Destroy this report when it is no longer needed. Do not return it to the originator.

ARL-TR-9879 ● FEB 2024

Resolution as a Computational Factor in CTH Simulations of a Shaped-Charge Jet

Daniel J Hornbaker
DEVCOM Army Research Laboratory

REPORT DOCUMENTATION PAGE

1. REPORT DATE	2. REPORT TYPE	3. DATES COVERED	
		START DATE	END DATE
February 2024	Technical Report	4/01/2023	10/31/2023

4. TITLE AND SUBTITLE
Resolution as a Computational Factor in CTH Simulations of a Shaped-Charge Jet

5a. CONTRACT NUMBER	5b. GRANT NUMBER	5c. PROGRAM ELEMENT NUMBER
5d. PROJECT NUMBER	**5e. TASK NUMBER**	**5f. WORK UNIT NUMBER**

6. AUTHOR(S)
Daniel J Hornbaker

7. PERFORMING ORGANIZATION NAME(S) AND ADDRESS(ES)	8. PERFORMING ORGANIZATION REPORT NUMBER
DEVCOM Army Research Laboratory ATTN: FCDD-RLA-TE Aberdeen Proving Ground, MD 21005-5069	ARL-TR-9879

9. SPONSORING/MONITORING AGENCY NAME(S) AND ADDRESS(ES)	10. SPONSOR/MONITOR'S ACRONYM(S)	11. SPONSOR/MONITOR'S REPORT NUMBER(S)

12. DISTRIBUTION/AVAILABILITY STATEMENT
DISTRIBUTION STATEMENT A. Approved for public release: distribution unlimited.

13. SUPPLEMENTARY NOTES
ORCID ID: Daniel J Hornbaker, 0000-0002-0746-1614

14. ABSTRACT
Uncertainty associated with resolution was investigated in CTH simulations of the formation of a 65-mm-diameter shaped-charge-jet laboratory device. Simulation outcomes varied in a consistent manner over a wide range of resolution, and several measured jet properties demonstrated limiting behavior, with 2-D and 3-D results converging to similar values. Estimates of the expected mean values and distribution widths for jet properties as a function of resolution were calculated. Jet mass variance due to discretization, resolution dependence of jet temperature, and observations of jet tip structure are also reported.

15. SUBJECT TERMS
numerical simulation, uncertainty quantification, CTH, shaped-charge jet, resolution study, Network, Cyber and Computational Sciences

16. SECURITY CLASSIFICATION OF:			17. LIMITATION OF ABSTRACT	18. NUMBER OF PAGES
a. REPORT	b. ABSTRACT	C. THIS PAGE		
UNCLASSIFIED	UNCLASSIFIED	UNCLASSIFIED	UU	30

19a. NAME OF RESPONSIBLE PERSON	19b. PHONE NUMBER *(Include area code)*
Daniel J Hornbaker	410-278-7697

STANDARD FORM 298 (REV. 5/2020)
Prescribed by ANSI Std. Z39.18

Contents

List of Figures

List of Tables

Acknowledgments

This work was performed as part of the Terminal Ballistics to Advance Army Modernization Priorities Frontier Project and supported in part by a grant of computer time from the Department of Defense (DoD) High Performance Computing Modernization Program (HPCMP) at the DEVCOM Army Research Laboratory (ARL) DoD Supercomputing Resource Center (DSRC).

This report marks the conclusion of a decade-long investigation into computational factors of simulation codes. This project would not have been possible without the availability of remarkable computing resources and the assistance of several capable experts. My gratitude extends to the following organizations and people.

It is difficult to overstate the impact of the HPCMP on defense research. By maintaining a centralized structure for high-performance computing across the DoD, the HPCMP enables critical defense work to be performed on multiple world-class systems across the nation in seamless fashion. It is undoubtedly one of the most successful DoD programs of the past half century. I thank the staffs of the various associated DSRCs who work diligently to maintain the supercomputing systems and promptly address issues as they occur.

ARL has long-standing productive relationships with the development teams at Sandia National Laboratories for both the ALEGRA and CTH codes. I would like to particularly thank Dr John Niederhaus for discussions involving the technical aspects and capabilities of ALEGRA.

I am grateful to the professional editors of ARL Technical Publishing I have worked with over the years to make these reports as clear, correct, and presentable as possible for the public.

Frontier Projects are an HPCMP program for advancing foundational research through the allocation of priority computing hours. Dr Robert Doney has been a primary leader of computational research in terminal ballistics at ARL through the submission of multiple successful Frontier Project proposals over the years.

In addition to possessing surpassing expertise in numerical modeling of terminal ballistics, Mr Stephen Schraml also builds the CTH code for use by ARL researchers across the many HPCMP supercomputing systems.

I am indebted to the now-retired Dr Steven Segletes for assistance in untangling how the simulation codes implement thermodynamic equations of state. I also thank Dr George Vunni for many helpful discussions and reviews over the years.

1. Introduction

Terminal ballistics simulations are routinely used in the development and evaluation of protection technologies for the US Army. Simulations are often cheaper, safer, and quicker to execute than the equivalent experiments. They can also reveal interactions and mechanisms that are difficult to observe in tests.

A great deal of information must be known about a system in order to accurately simulate it, beginning with the geometry, composition, and initial motion of all objects. Strength and thermodynamic models are typically required for each material involved. There are also many parameters relating to the computational structure and numerical methods of a simulation, which I will refer to collectively as *computational factors*. These include such things as choice of code and supercomputing system, the spatial extent covered by the simulation, the allowed time step durations and simulation stopping conditions, the size of computational domain elements, and so forth.

A typical difficulty in experimental science is an inability to accurately control or precisely measure important system parameters. Numerical computations present the opposite problem as users are required to specify exact values for every simulation parameter. Ballistic test data can be used to determine some parameter values, but this requires care as the large number of parameters involved often means that simulations can be made to match any particular outcome by the computational equivalent of overfitting, meaning simulations will accurately reproduce known results while having little ability to predict new data. For this reason, a preferred approach to fixing parameters is via characterization methods unrelated to the problem of interest. For example, material models and associated parameters are often derived from basic nonballistic engineering tests of material behavior. In cases where appropriate parameter values remain ambiguous, users may run ensembles of simulations over a sampling of plausible values to generate a range of possible outcomes.

While selection of material models and determination of their parameters receives a fair amount of attention in the literature, discussions of computational factors are often limited to *resolution*, which refers to the size of discrete computational elements. A typical assumption is that finer resolution (i.e., smaller elements) leads to more accurate simulation outcomes. Resolution studies often focus on estimating the tradeoff between accuracy and the rapidly increasing computational cost that comes with finer resolution.

How parameter values are selected for other types of computational factors is discussed less often. Some choices may be practical (e.g., which simulation code is available and familiar to the user). Other parameters may be selected arbitrarily or

by habit (e.g., orientation of a problem within a simulation). Still other parameters may simply rely on code defaults (e.g., time step control parameters).

After encountering examples of surprisingly large changes in simulation results tied to seemingly negligible parameters, I became interested in studying the influence of computational factors on simulation outcomes. This report concludes a series of investigations into uncertainty in numerical simulations that I began in 2015. Two different codes developed at Sandia National Laboratories, CTH and ALEGRA, were selected for study. The intent was not to put them in competition against each other, but to highlight the fact that variability begins with choice of code. The methodologies developed over the course of this work should be equally applicable to other multi-physics codes used to simulate terminal ballistic events.

While the primary focus has been on measuring variability due to computational factors, my reporting over the years has included much ancillary material intended to serve the interests of several different audiences. The specific results are directly relevant to users of CTH and ALEGRA, two codes that have a long history of use within the protection community. For numerical modelers in general, measuring the influence of computational factors on simulation outcomes draws attention to these sometimes overlooked parameters and suggests a methodology for how to test their influence in other applications. For researchers who are relatively new to numerical simulations, I have included detailed discussions of equations of state and constitutive models to provide helpful points of entry to these topics. I meticulously sourced the parameter values for the material models used in this project as much as possible, rather than appealing to the common expedient of vaguely crediting code material libraries or models borrowed from prior work, to highlight the invaluable effort that goes into developing material models.

Some sections of these reports were written to serve as brief primers on important topics relating to numerical modeling. These are aimed at decision makers who regularly encounter, but are not necessarily expert in, simulation data. Understanding some of the fundamental aspects of numerical modeling can aid in judging the capabilities and limitations of simulations and provide greater confidence in evaluating data.

Finally, open publication of this research serves a civil purpose by making accessible to the US public an example of how taxpayer investment in the HPCMP benefits our nation. Much research in protection technology must necessarily be withheld from the public for reasons of national security. The fundamental nature of this project allows the public an opportunity to glimpse the sorts of activities involved in the research of protection technologies.

2. Project Synopsis

The initial report[1] began with a broad overview of numerical modeling and outlined the scope of the project. In this first investigation of the influence of computational factors on simulation outcomes, a simple terminal ballistics problem of a rod penetrating a steel target block was examined. Depth of penetration (DoP) into the target was the primary quantity of interest used to measure outcome variability in CTH and ALEGRA simulations of this model system. The main finding was that while simulations produce mathematically different outcomes when most of the tested computational factors were varied, the differences were often insufficient to change DoP by more than the measurement threshold limit imposed by the 0.5-mm resolution of the simulations. This DoP insensitivity was unsurprising given the simplicity of the model system, but establishing the methodology was an important step in the project. Also of value was the demonstration that simulation run times could vary appreciably as a result of computational factors, which is an important consideration for projects requiring large numbers of simulations.

The second investigation[2] applied the same series of tests used in the first study to the more complex problem of a shaped-charge jet (SCJ) penetrating a steel target block. Unlike for the simple rod problem, DoP values in this model system varied by measurable amounts. Many computational factors produced DoP variances between 2% and 4% of the mean value in CTH simulations. Variances in ALEGRA were generally smaller, ranging from 0.5% to 1.5% of mean value, but at a cost of significantly longer run times for equivalent simulations. These results demonstrated the approximative nature of numerical simulations, which have an irreducible level of uncertainty in outcomes distinct from that which might be attributable to variations of material models or geometric tolerances of objects.

The third investigation[3] focused on the effects of resolution. While cursory resolution tests were conducted in the prior stages of the project, for most of the work the resolution was fixed at 0.5 mm. A simple toy model was presented to illustrate the special role of resolution in simulations. This study examined the effects of varying resolution in ALEGRA simulations of the initial 40-μs formation stage of the SCJ model developed in the prior report. It was seen that ALEGRA produces generally monotonic behavior of various bulk SCJ properties such as total kinetic energy and total axial momentum as resolution decreases toward zero. The extrapolated limiting values of these properties in 2-D simulations are closely matched to those in the 3-D case. The underlying cause of excessive heat development in simulations of SCJs was also revealed to be driven by resolution, with jet temperature decreasing substantially as resolution becomes finer.

A fundamental expectation of numerical simulations is that as resolution is reduced to zero, outcomes should converge upon the unique solution to the underlying

continuum problem that the simulation is based on. This implies that variances in simulation outcomes should also vanish as resolution approaches zero since the continuum problem has a single fixed solution. Thus, the variances due to computational factors measured in the first two reports are specifically linked to the fixed 0.5-mm resolution used in those investigations. These variances can be expected to change with resolution. An ad hoc method for estimating the expected variance of SCJ properties as a function of resolution was developed.

A supplemental study[4] was performed to follow up on open questions arising from the third stage of the project. The main task was to directly test the ad hoc method for estimating expected variance as a function of resolution. Ensembles of randomized 2-D simulations at several fixed resolutions were performed. The resulting outcome distributions were generally within the estimated expected variance produced using the ad hoc method, though variances at coarse resolutions were much smaller than predicted. Two other topics also received additional study. Unphysically fragmented jet tip morphologies seen at high resolution were shown to be attributable to the threshold fracture pressure parameter within the ALEGRA void insertion model. There was also evidence that this fragmentation may be a transient effect appearing only over a fixed range of resolution. Finally, limiting the size of time steps while holding resolution fixed was shown to increase the mass-average SCJ temperature, which indicates that the overall decrease of temperature with decreasing resolution must be driven by spatial effects that dominate temporal ones.

In this final report, the resolution study of third investigation is repeated using the CTH code. The SCJ formation model is reviewed in Section 3, and computational details of the study are provided in Section 4. Section 5 contains the results and analysis of this work, followed by concluding remarks in Section 6.

3. Model System

The previously employed model[2] for the laboratory 65-mm-diameter precision SCJ device (Fig. 1) was used for this investigation. Changes made to the original model for the previous ALEGRA study[3] were applied here as well. The explosive is detonated from a point at the center of the back face rather than from the entire plane, making the detonation wave front spherical rather than planar. The Johnson–Cook fracture model was not used for the copper liner material, following suggestions in work by Schraml.[5] All other aspects of the material models for the copper liner and explosive are unchanged from the original.[2]

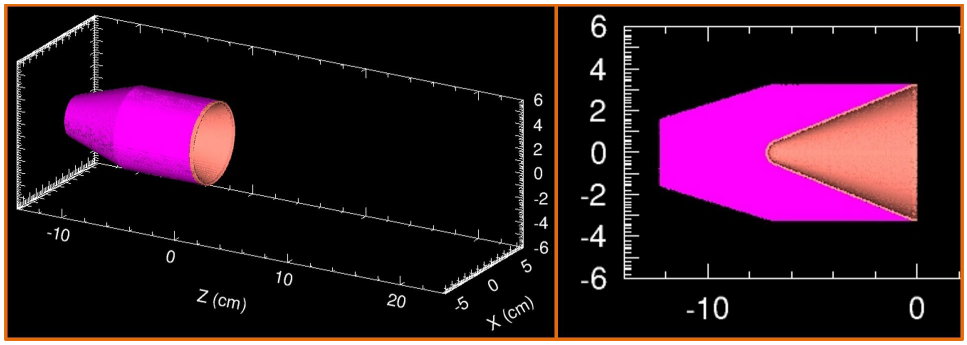

Fig. 1 Perspective (left) and section (right) views of the 65-mm SCJ device model

4. Computational Setup

Simulations were performed on a TI-20 Linux HPC Cluster supercomputer with hostname JEAN located at the US Army Combat Capabilities Development Command (DEVCOM) Army Research Laboratory (ARL) and managed by its Department of Defense Supercomputing Resource Center (DSRC). JEAN features 407 standard compute nodes with Intel Xeon Platinum 9242 processors operating at 2.3 GHz. Each node has 96 compute cores.

Some data analysis was performed using an HPE SGI 8600 supercomputer with hostname KOEHR located at the John C Stennis Space Center and managed by the US Navy DSRC. KOEHR has 704 standard compute nodes featuring dual 2.7-GHz Intel Xeon Platinum 8168 24-core processors and 170 GB of memory.

In total, one hundred and two 2-D resolution simulations, ninety-five 3-D resolution simulations, and sixty 3-D decomposition test simulations were completed. The total computing time amounted to approximately 2.6 million core-h.

4.1 Decomposition Study

An aspect of CTH code performance noted in past work is variability in outcomes based on how a problem is divided among the available cores, which is referred to as problem decomposition. This behavior was first observed in the initial work on the simple rod impact problem,[1] with some discussion of the issue appearing in Sections 5.2 and 5.3 of the following report.[2] The rod impact problem has since been used to test decomposition in new versions of CTH as they become available on different supercomputing systems.

Table 1 shows results from decomposition testing. Results for CTH version 11.1 on HERCULES appears in Table 12 of the first project report.[1] Platform specifications for HERCULES and EXCALIBUR also appear there.[1] Those for CENTENNIAL can be found in the third report.[3]

Table 1 CTH decomposition testing results for various versions and platforms

Platform			HERCULES		EXCALIBUR		EXCALIBUR	
CTH Version			11.1		12.0		12.1	
DoP (cm)			8.69–8.70		8.72		8.72	
Decomposition			Cycles	Run Time (h)	Cycles	Run Time (h)	Cycles	Run Time (h)
X	Y	Z						
4	4	4	7771	17.8	7847	17.4	7840	14.9
1	1	64	7812	22.6	7851	28.7	7860	26.2
1	64	1	7816	27.8	7855	36.0	7849	34.0
64	1	1	7812	34.6	7849	41.8	7849	40.0
2	2	16	7810	15.1	7850	16.7	7846	14.4
2	16	2	7813	16.9	7847	17.1	7859	14.7
16	2	2	7811	20.9	7852	20.8	7851	18.5
1	8	8	7811	16.5	7850	16.8	7855	14.4
8	1	8	7815	19.1	7851	18.7	7849	16.0
8	8	1	7810	16.0	7847	16.2	7848	13.6

Platform			CENTENNIAL		CENTENNIAL		JEAN	
CTH Version			12.1		12.2		12.2	
DoP (cm)			8.72		8.71		8.72	
Decomposition			Cycles	Run Time (h)	Cycles	Run Time (h)	Cycles	Run Time (h)
X	Y	Z						
4	4	4	7847	12.9	9563	17.4	9644	10.4
1	1	64	7863	18.9	9563	23.8	9644	14.7
1	64	1	7855	21.3	9563	25.9	9644	17.8
64	1	1	7849	28.4	9563	35.6	9644	21.4
2	2	16	7859	13.2	9563	16.6	9644	10.1
2	16	2	7848	12.9	9563	16.6	9644	10.4
16	2	2	7847	16.9	9563	21.7	9644	12.8
1	8	8	7850	12.7	9563	16.4	9644	10.1
8	1	8	7846	14.7	9563	18.9	9644	11.7
8	8	1	7849	11.8	9563	15.6	9644	9.7

While CTH code builds continued to exhibit variability due to decomposition through version 12.1, builds of the current version 12.2 proved decomposition invariant on both CENTENNIAL and JEAN, removing this factor as a source of outcome variability in this current study. Run times on JEAN are also substantially faster than on previously tested platforms despite an increase in the number of cycles required for simulations to reach completion.

4.2 Simulation Parameters

The remaining simulations in this report were performed using version 12.2 of the CTH code.[6] Both the 2-D and 3-D computational domains were constructed as in the previous ALEGRA study.[3] With varying resolution, each simulation has a slightly different spatial extent. Domains were structured with the minimum number of cells that satisfied the following criteria:

- The coordinate origin was coincident with a mesh node.
- The coordinate origin was set along the centerline of the SCJ device (y-axis in 2-D, z-axis in 3-D) at the end of the copper liner.
- The domain extends at least 6 cm in each lateral direction.
- The domain includes the span from –14 cm to 24 cm along the axis.

Apart from the axial symmetry boundary at $y = 0$ in 2-D simulations, all domain boundaries were set to vacuum outflow. Cell volumes not occupied by copper or explosive from the SCJ device were void space.

Material discards helped ensure simulations would reliably run to completion. All material with temperature over 10,000 K or specific internal energy less than –100 kJ/g was discarded. Low-pressure explosive reactant was removed by discarding explosive material having pressure less than 101,325 Pa (1 atm) and density less than 0.05 g/cm^3.

Simulations were run to 40 μs. Image plots of various jet properties were generated in 1-μs intervals using the integrated Spymaster capability.[7] The computational domain was exported in the Exodus II format[8] every 5 μs, though the export at 5 μs was skipped as the detonation wave does not yet reach the liner at that time.

4.3 Project Workflow

Simulations were run at 0.999-mm resolution, then in 0.10-mm increments from 0.990 mm down to the smallest resolution that would run to completion in less than 168 h on no more than 50 nodes. For 3-D simulations the smallest resolution that could be run was 0.060 mm. 2-D simulations could be run down to 0.010 mm, with additional simulations at 0.005 and 0.003 mm completed as well.

An automated workflow similar to that in the ALEGRA study was used.[3] Jobs were scheduled on JEAN with Slurm[9] version 23.02. Cell data were extracted from the Exodus exports using ParaView[10] version 5.11.0. For each cell containing a volume fraction of copper greater than 1E-16, the material volume fraction, mass, velocity vector, pressure, temperature, and specific internal energy were extracted with 7 digits of precision. All quantities in CTH are exported as element-centered data.

Data analysis was performed using MATLAB release R2023a (MathWorks, Inc.). After simulation parameters were extracted from the process files, data at each recorded time were processed in sequence. Exported element data were read and derived quantities calculated. Derived element quantities are density, total velocity magnitude, radial distance from the z-axis, and radial velocity magnitude. All data were then written out in MATLAB matrix data format for storage.

A variety of jet characteristics were then calculated and plotted. Examples include distributions of mass as a function of material density, pressure, temperature, axial position, and radial position; distributions of mass, specific internal energy, kinetic energy, and mass-averaged temperature as a function of material axial velocity; a reverse cumulative mass distribution of the jet as a function of axial velocity (referred to as a VjM plot)[5]; and global scalar values including total mass, total kinetic energy, and total axial momentum. Also of interest is the thermodynamic state values at the locus of maximum jet material pressure (referred to as the "pressure center" from here on).

Upon completion of the analysis, the postprocess script collected all process scripting, input files, and output data for transfer and long-term archiving.

5. Results and Discussion

The amount of data generated in these simulations is too copious to completely document here. A selection of results highlighting a few specific topics of interest is provided instead.

5.1 Computational Time

One direct measure of the cost to run a simulation is the computational time (Fig. 2), which is the elapsed real run time multiplied by the total number of cores used. Computational time T_C for 2-D simulations at coarse resolutions r were dominated by code start-up and data read/write operations, with real run times only slightly increasing from 41 s at r = 0.999 mm (T_C = 1.093 core-h) to 44 s at r = 0.600 mm (T_C = 1.173 core-h). At finer resolutions T_C scales approximately as the inverse of r raised to the power 3. A good fit to the measured computational times is given by

$$T_C^{(2\text{-}D)} = 1.093 + \frac{0.01245}{r^{3.038}}. \quad (1)$$

Computational time for 3-D simulations was fit with an equation of the same form,

$$T_C^{(3\text{-}D)} = 4.098 + \frac{5.859}{r^{4.144}}. \quad (2)$$

The exponent values in these curve fits follows the expected scaling of approximately the number of spatial dimensions plus one.

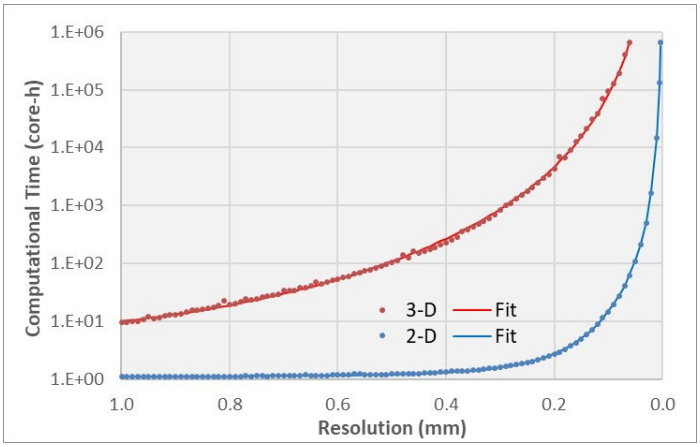

Fig. 2 Computational time (log scale) vs. resolution

The computational time of a simulation can also be compared with the overall size of the simulation S_C as measured by total element-steps taken, which is the number of domain elements multiplied by the number of time steps taken to reach the simulation stop time (Fig. 3). T_C becomes proportional to S_C once simulations reach an appreciable size. The ratio provides a measure of performance for the hardware and build of the code. Comparing the performance of 2-D and 3-D simulations shows that element-steps in 3-D take a factor of 1.45 longer to compute:

$$T_C^{(2\text{-}D)} = 0.57\, S_C^{1.000}, \tag{3}$$

$$T_C^{(3\text{-}D)} = 0.82\, S_C^{1.029}. \tag{4}$$

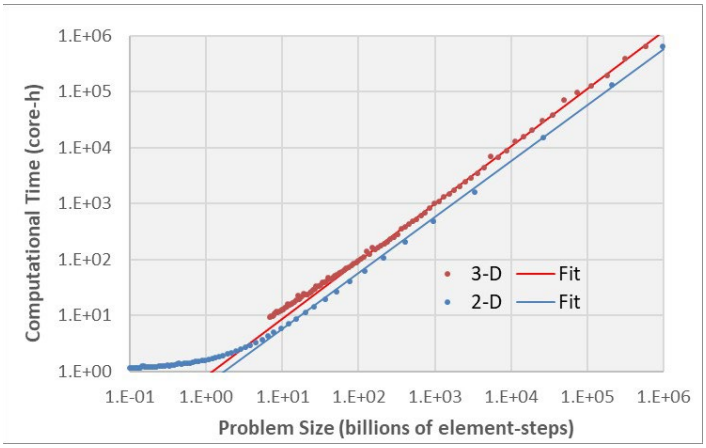

Fig. 3 Log-log plot of computational time vs. problem size

5.2 Total Liner Mass

Objects are inserted into the domain at the start of a simulation via the space-filling DIATOM routine. Descriptions of geometric boundaries are used to determine which elements are filled with material. For elements intersecting a boundary surface, the ITERATION parameter specifies the number of times that element is

subdivided to estimate the amount of material volume it contains. ITERATION was set to 5 for all simulations.

The DIATOM process produces some small variability in total object mass. The initial total mass of the copper liner at each resolution is plotted in Fig. 4. At coarse resolutions, the mass varies more for 2-D simulations than those in 3-D. This is attributable to the underlying differences in domain geometry. Elements in 2-D simulations represent annuli, and the volumes associated with these elements increase with distance from the axis. In contrast, 3-D elements are identical cubes with a fixed volume much smaller than a 2-D element at the same resolution. Consequently, small variances in the filling of 2-D elements will have greater effect on total mass than corresponding variances in the filling of 3-D elements. As the resolution becomes finer, differences in initial total mass between 2-D and 3-D simulations narrow as both approach the continuum limit of 79.482 g.[3]

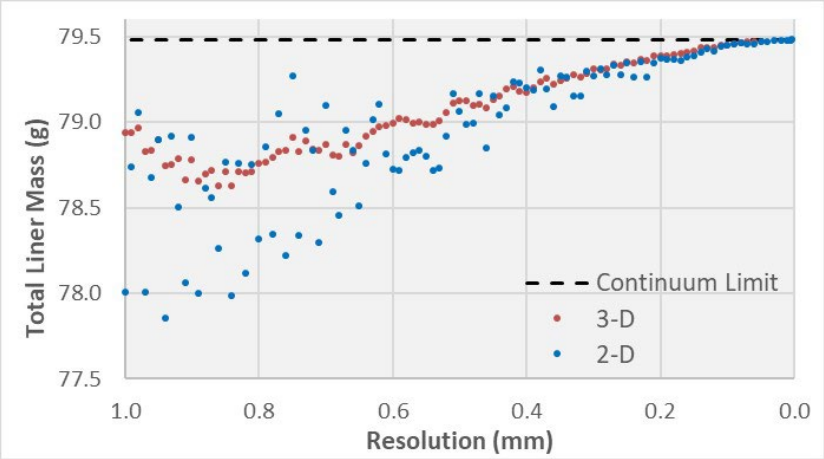

Fig. 4 Total liner mass vs. resolution at 0 μs

During a simulation, mass can be lost either by exiting the domain or by triggering one of the material discard conditions discussed in Section 4.2. Measurable liner mass loss (at least 0.0001 g) at 40 μs was seen in twelve 2-D simulations and twenty-two 3-D simulations. The 2-D simulation at 420-μm resolution showed a loss of 0.0001 g at 20 μs, but a regain of that loss at 25 μs, which likely reveals the size of round-off errors in the mass calculations.

Liner mass losses greater than 0.0001 g were measured in eight 2-D simulations and one 3-D simulation. The 3-D simulation at 0.999-mm resolution had a 0.0002-g mass loss at 40 μs due to small particles exiting the domain. The 2-D simulations at and below 0.060-mm resolution exhibited larger mass losses ranging from 0.0006 to 0.0171 g. While mass losses affect calculations of extrinsic jet properties such as total momentum and total kinetic energy, these losses are significantly smaller than the variations in total initial liner mass seen in Fig. 4 and are therefore treated as negligible.

5.3 Jet Temperature

As was seen in ALEGRA simulations,[3,4] the temperature of the jet depends strongly on resolution. A simple means of reducing the complex temperature profiles of a jet to a single scalar value is through mass averaging, in which the temperature of the material in each element is multiplied by the mass within that element, then the total sum of these values is divided by the total liner mass. A plot of the mass-average temperature $\bar{T}$ (Fig. 5) reveals more heat developing during jet formation at coarse resolutions.

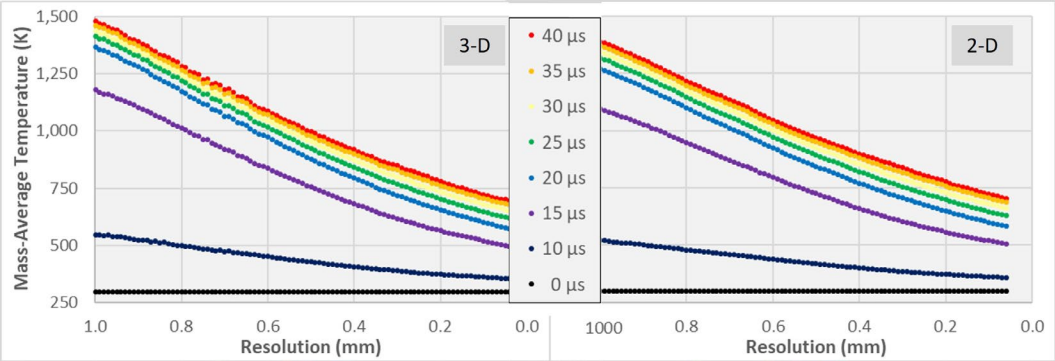

Fig. 5 Mass-average temperature vs. resolution at various times in 3-D (left) and 2-D (right) simulations

The resolution dependence of $\bar{T}$ is directly attributable to the thermodynamic conditions in the region of maximum pressure in the collapsing liner, which will be referred to as the "pressure center" (previously labeled "pressure head" in the prior ALEGRA report, but changed here to avoid conflict with a preexisting unrelated definition for that term in fluid dynamics). The pressure center at each time step is defined as being located in the element having the largest liner material pressure, with the restriction that it must radially be within two resolution lengths of the jet axis and must contain a volume fraction of copper greater than 0.5.

The location of, and thermodynamic conditions at, the pressure center change throughout the jet formation process. The overall maximum pressure in a jet is attained sometime between 10 and 20 µs. The material pressure, density, and temperature at the pressure center at 15 µs are plotted in Fig. 6 as a function of resolution. The correspondence between the temperature at the pressure center and $\bar{T}$ of the resulting jet is clear.

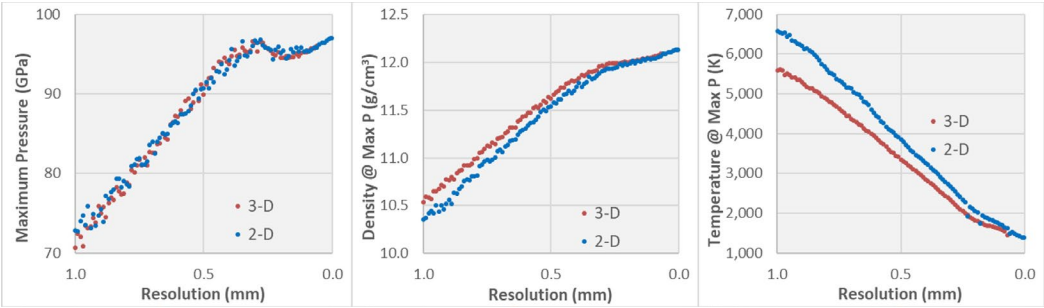

Fig. 6 Maximum pressure (left) along with the associated density (center) and temperature (right) vs. resolution at 15 μs

5.4 Jet Tip

The evolution of the jet tip shape is indicative of resolution effects on overall jet structure. Images of the jet tip at 40 μs in 3-D and 2-D simulations as resolution varies are shown in Fig. 7. Note that black lines in 2-D images are image artifacts, not voids in the material.

A slightly thickened end region appears as resolution becomes finer. A shroud of detached particles begins to form by 0.500 mm in 2-D and 0.400 mm in 3-D. In the cylindrical 2-D geometry, the particles of detached material represent annular rings. Since these rings cannot break apart in 2-D, they stretch and thin out. In contrast, 3-D geometry allows angular particulation, though the size and orientation of the particles are strongly dependent on the domain structure.

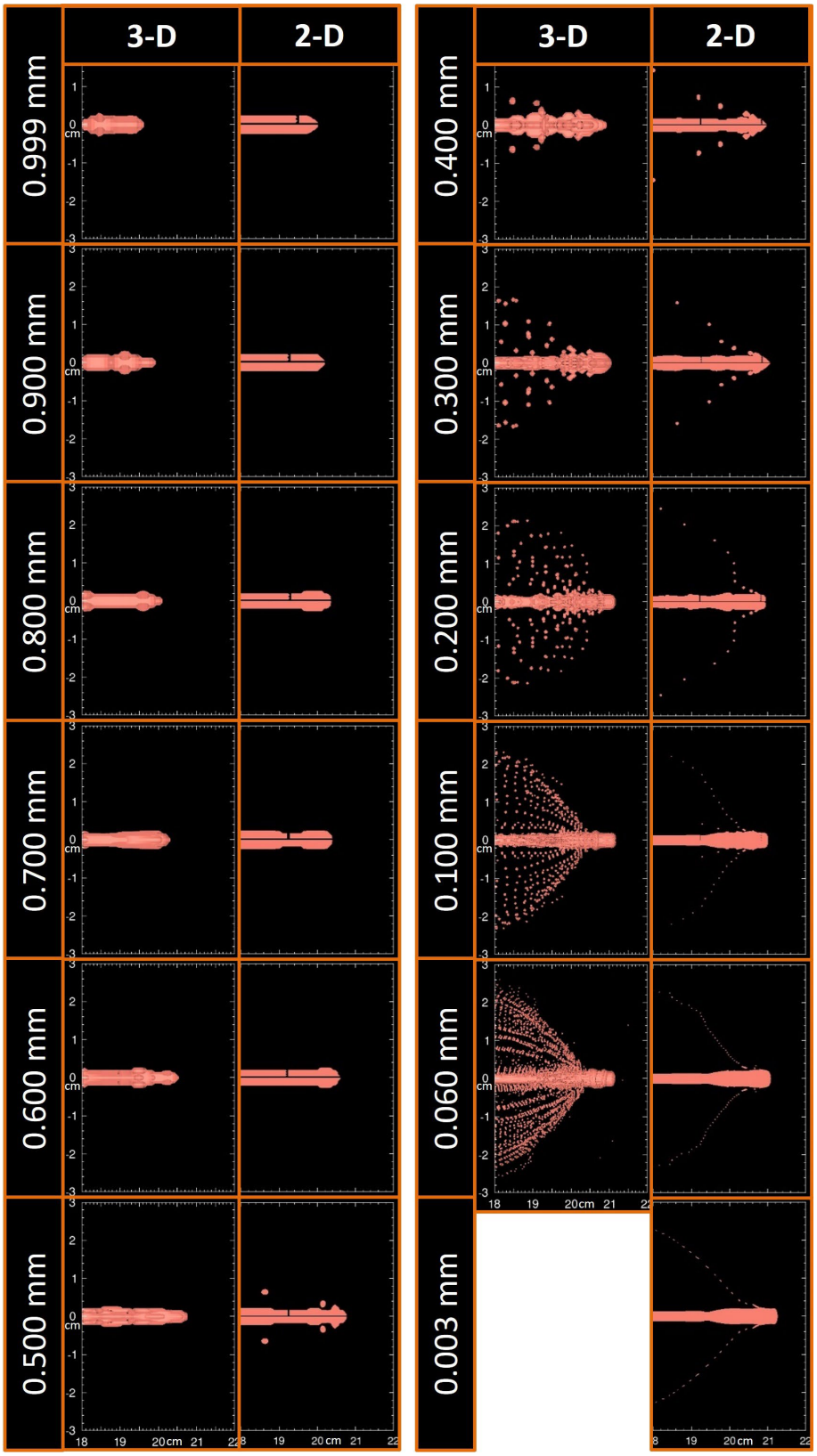

Fig. 7 Jet tip at 40 μs in 3-D (left) and 2-D (right) simulations at various resolutions

The changing position of the tip shows that the velocity is generally increasing as resolution becomes finer. Tip velocity was measured in simulations (Fig. 8) by finding the maximum z-velocity among cells near the axis having the largest z-coordinate. Cells near the axis are those within 1 cm radially of the z-axis. This is an instantaneous velocity, which can include transient effects due to material deformations, shock waves, and elastic/plastic flow that would average out over longer time scales.

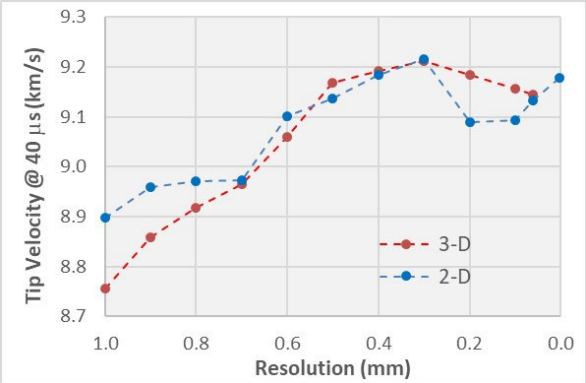

Fig. 8 Tip velocity vs. resolution at 40 μs

Tip velocities in 2-D and 3-D simulations are within 100 m/s of each at most resolutions. Simulations at coarse resolution have tip velocities below 9 km/s, while velocities settle between 9.1 and 9.2 km/s at resolutions finer than 0.600 mm.

5.5 Jet Mass at High Velocity

One way to characterize a jet is by measuring its cumulative mass as a function of decreasing axial velocity—in other words, at any given velocity, how much jet mass has an axial speed equal or greater than that velocity. A graph of such data is referred to as a V_jM plot.[5] Figure 9 shows V_jM data for 2-D and 3-D simulations at 40 μs with various resolutions. To construct this plot, jet mass was sorted into velocity bins 25 m/s wide and cumulatively summed from high to low velocity.

Data at 4 km/s show that even in coarsely resolved simulations, jets have nearly all the high-velocity mass they project to have in the continuum solution. The total jet mass with velocity at least 4 km/s increases by less than 5% from the coarsest resolution of 0.999 mm down to the finest attainable resolutions.

The main effect of decreasing element size is a shift of mass downstream from the base of the jet toward the tip. At the highest velocities, the V_jM plots clearly show an increasing tip velocity as resolution is lowered to around 0.600–0.500 mm, as previously documented in Fig. 8. As resolution becomes finer, the data show the mass at the highest velocities increasing from near 0 g to almost 2 g, consistent with the tip thickening seen in Fig. 7.

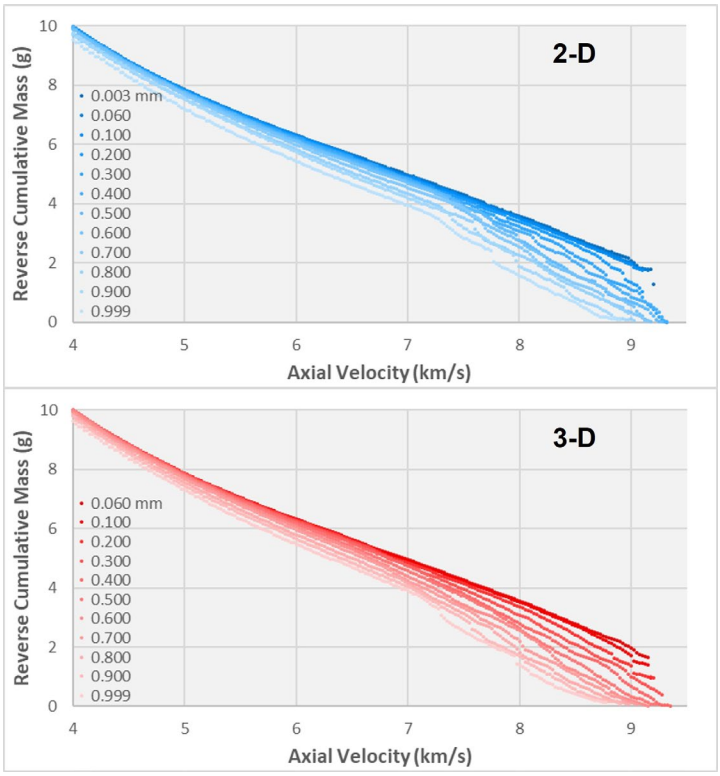

Fig. 9 V_jM data at 40 μs for 2-D (top) and 3-D (bottom) simulations at various resolutions

5.6 Resolution-Dependent Numerical Uncertainty

The material states of a jet vary considerably from tip to tail and core to skin. Elucidating the ways in which a simulated jet changes with resolution is challenging. One expedient is to reduce the jet to a set of sum-total properties, such as total kinetic energy, total internal energy, mass-average temperature, and total axial momentum.

At any fixed resolution, such values form a distribution as other computational factors (e.g., symmetry, translation, and origin placement) are varied. As demonstrated previously,[4] these distributions can often be treated as normal, with an associated mean value and a width expressed as a standard deviation, which provides a measure of the uncertainty for that jet property.

These distributions change with resolution. The reason why resolution stands apart from other computational factors is that as resolution goes to zero, the simulation outcomes converge upon the unique solution to the underlying continuum problem. Accordingly, distributions of jet properties must converge to the values associated with the continuum solution, and the associated standard deviations must vanish.

Determining how jet property distribution means and standard deviations change with resolution is a core aim of this work. As was demonstrated in the previous report,[4] directly constructing jet property distributions at multiple resolutions is

prohibitively costly. It would be preferable to obtain the desired information directly from resolution series data. An ad hoc method for doing so was previously developed,[3] based on the idea that the jet property values at each resolution can be treated as random selections from the associated distributions. Inspection of jet property value versus resolution plots shows this presumption is clearly false as the data exhibit a smoothness indicative of correlated (i.e., nonrandom) outcomes. Obtaining randomized results would entail randomly shuffling all the relevant computational factors as resolution varied, which was not done for these resolution series. Even so, the ad hoc method can be applied to the available data to generate estimates for the expected distribution mean values and standard deviations as functions of resolution. Strictly speaking, this is an improper application of statistics, but prior results[4] suggest that the resulting standard deviation estimates provide an upper bound on actual measured distribution widths.

A condensed review of the ad hoc method follows. It begins by fitting the measured jet properties as a function of resolution *r*. Data in these simulations are amenable to quadratic function fits,

$$F(r) = Ar^2 + Br + C, \tag{5}$$

with fitting parameters [*A*, *B*, *C*]. This function is taken to be an estimate of the mean value of the associated property as resolution varies. Note that this implicitly assumes that mean values of jet properties are continuous functions of resolution. The value of the *C* parameter is an estimate for the jet property value in the continuum limit.

To estimate the distribution width at each resolution, bounding curves of the same quadratic form are used,

$$F^{\pm}(r) = (A \pm A_\sigma)r^2 + (B \pm B_\sigma)r + C, \tag{6}$$

with fitting parameters [A_σ, B_σ] selected so that approximately 68% of the data, corresponding to percentage of a normal distribution within 1 standard deviation of the mean, are within the bounds. As with the mean-estimate curve fit, this assumes that distribution width is a continuous function of resolution. Non-uniqueness in choice of fitting parameters is resolved by maximizing the number of runs between in-bound and out-of-bound data, though in all cases the data fail a statistical test of run randomness,[3] which is expected given the data are already known not to be properly random.

An estimate of the uncertainty due to computational factors as a function of resolution can now be made. At any resolution *r*, the estimated standard deviation $\sigma(r)$ of the jet property distribution is

$$\sigma(r) = F^{+}(r) - F(r) = A_\sigma r^2 + B_\sigma r. \tag{7}$$

The estimated coefficient of variation CoV due to computational factors at a given resolution r is then

$$CoV = \frac{\sigma(r)}{F(r)}. \tag{8}$$

Results of this analysis for the jet properties listed at the beginning of this section are summarized in Table 2.

Table 2 Estimated mean value and σ for various jet properties at 40 μs

Jet property at 40 μs		Mean value estimate $A\,r^2 + B\,r + C$				σ estimate $A_\sigma\,r^2 + B_\sigma\,r$		CoV at r = 0.500 mm (%)
		A	B	C	R^2	A_σ	B_σ	
Total kinetic energy (kJ)	2-D	–34.311	–9.552	304.839	0.9955	0.000	1.865	0.32
	3-D	–20.513	–28.503	307.219	0.9995	0.000	0.717	0.12
Total internal energy (kJ)	2-D	13.448	15.928	21.592	0.9993	0.000	0.458	0.69
	3-D	10.153	15.815	21.548	0.9998	0.218	0.120	0.36
Mass-average temperature (K)	2-D	347.820	478.388	672.356	0.9994	0.000	13.355	0.67
	3-D	255.067	477.030	670.134	0.9997	5.800	3.900	0.35
Total axial momentum (N)	2-D	–13.150	12.900	128.484	0.8930	0.000	0.743	0.28
	3-D	–9.422	9.094	128.769	0.9130	0.000	0.481	0.18

Comparing the estimated continuum limit values (the C fit parameter) for jet properties in Table 2 with the previously obtained values using the ALEGRA code[3] shows how choice of code functions as a computational factor (Table 3). While the simulations in both codes represent the same basic continuum problem and are constructed as equivalently as possible, the codes produce different estimates for the jet properties of the continuum solution. For this jet formation problem, the differences between the codes are mostly negligible, though the mass-average temperature difference is notable and possibly worth additional investigation. Taking a broader perspective, for problems of sufficient importance, a way of accounting for code-based uncertainty is to run simulations using multiple codes and aggregating the results. Such multimodel ensembles are currently employed in climate change modeling and hurricane path prediction.

Table 3 Estimated continuum limit values for various jet properties at 40 μs

Jet property at 40 μs		Estimated limiting value (fit parameter *C*)	
		CTH	ALEGRA
Total kinetic energy (kJ)	2-D	304.8	310.5
	3-D	307.2	312.3
Total internal energy (kJ)	2-D	21.6	22.5
	3-D	21.5	22.8
Mass-average Temperature (K)	2-D	672.4	699.4
	3-D	670.1	704.9
Total axial Momentum (N)	2-D	128.5	131.0
	3-D	128.8	132.0

Examining each jet property in turn, total kinetic energy in 3-D simulations exhibit strong regularity with resolution (Fig. 10). More scatter is seen in the data for 2-D simulations, particularly at coarse resolution. Some of this scatter is directly attributable to geometric variance; dividing total kinetic energy by the total liner mass (Fig. 4) noticeable smooths the data (Fig. 11).

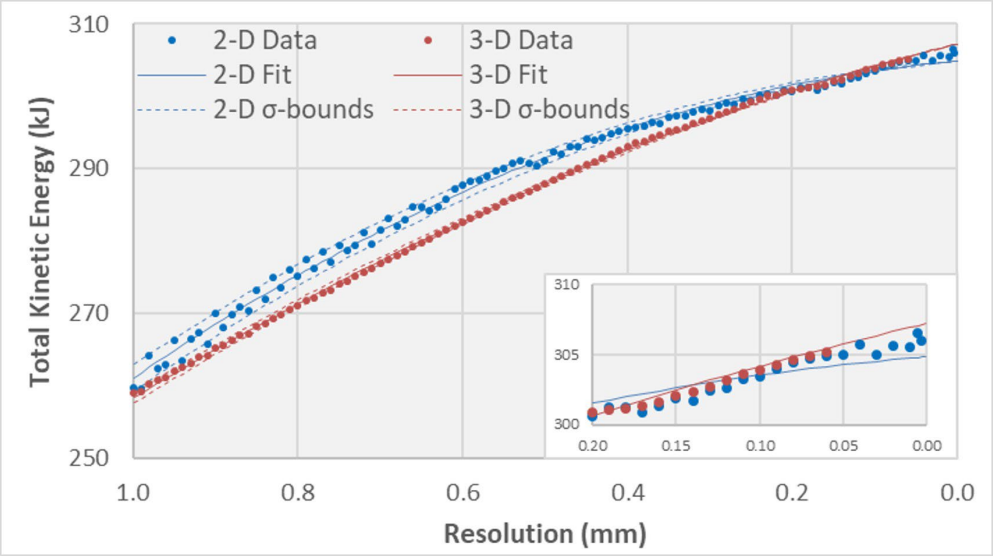

Fig. 10 Total kinetic energy vs. resolution at 40 μs

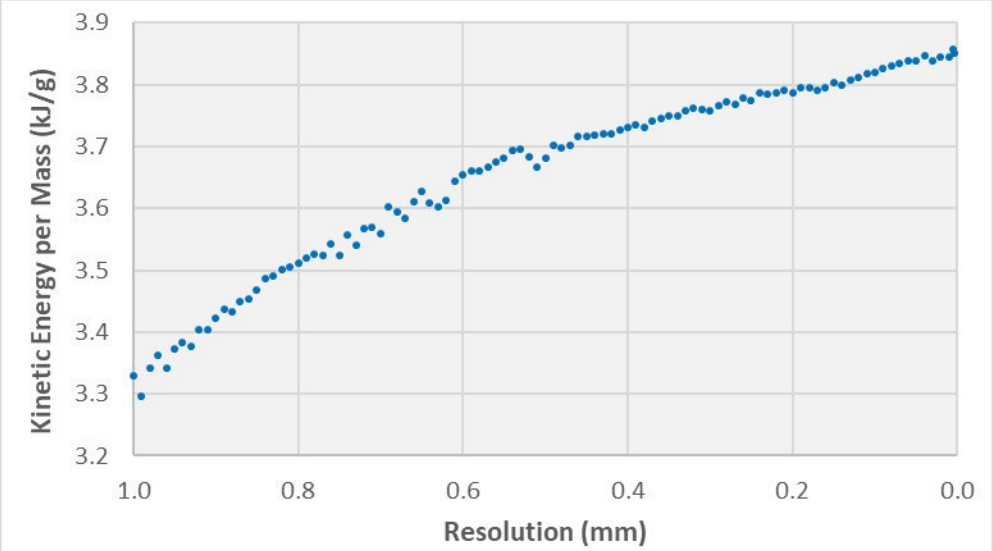

Fig. 11 Kinetic energy per unit mass vs. resolution for 2-D simulations at 40 μs

The 2-D and 3-D data are closely aligned at high resolution (Fig. 10 inset). The 2-D results have some scatter at resolutions of 0.050 mm and below, where 3-D simulations were not practical to run. In addition to the expectation that both 2-D and 3-D simulations should converge upon fixed values in the continuum limit of 0-mm resolution, in principle they should converge to the same value, namely the

total kinetic energy associated with the unique solution of the continuum problem. The curve fits for the data provide two different estimates of that value.

The alignment between 2-D and 3-D results at high resolution is even more pronounced for total internal energy (Fig. 12) and mass-average temperature (Fig. 13). While not strictly identical, these two properties are closely related. The strong dependence of jet temperature with resolution is discussed in Section 5.3.

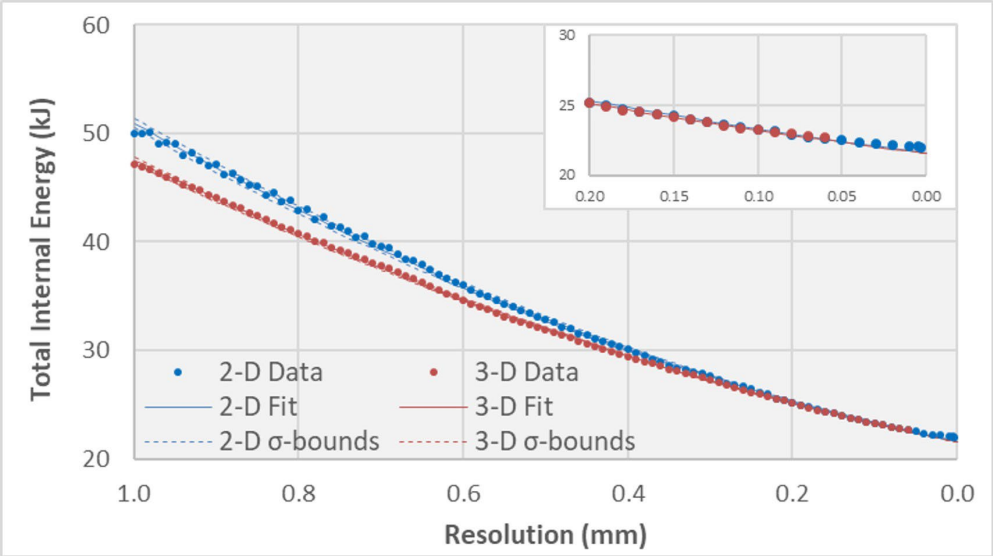

Fig. 12 Total internal energy vs. resolution at 40 μs

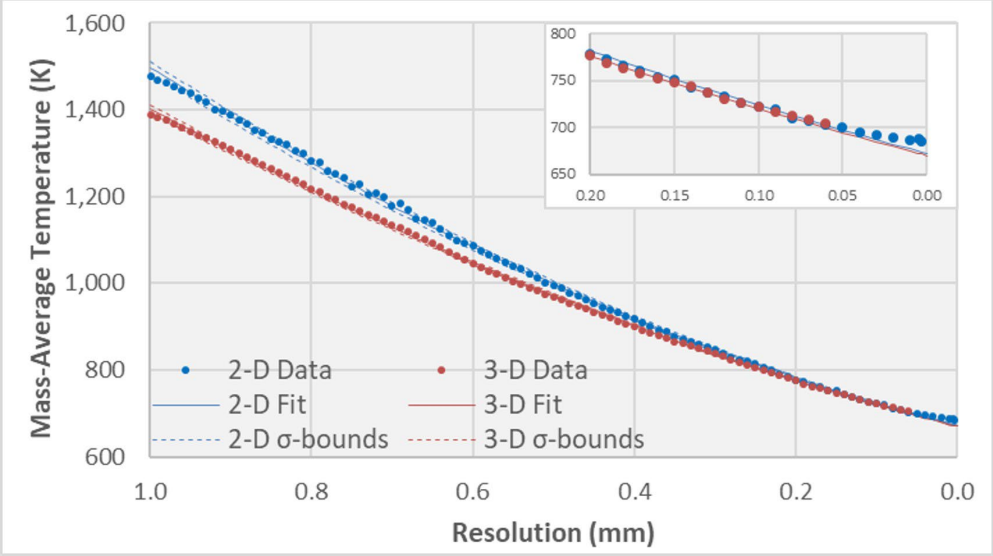

Fig. 13 Mass-average temperature vs. resolution at 40 μs

In contrast with the previous jet properties, total axial momentum shows a non-monotonic dependence on resolution (Fig. 14), with values first increasing as resolution becomes finer before falling off as resolution approaches zero. Scatter in the data is also more pronounced than for other properties. Comparison with the V_jM data plotted in Fig. 9 suggests that the increasing momentum corresponds with the driving of jet mass to higher velocity. Axial momentum levels off in the same range of resolutions that tip velocity attains its maximum value. While the mass of the tip increases at finer resolutions, the overall axial momentum of the jet decreases, despite the fact that total kinetic energy generally increases throughout the full resolution range (Fig. 10).

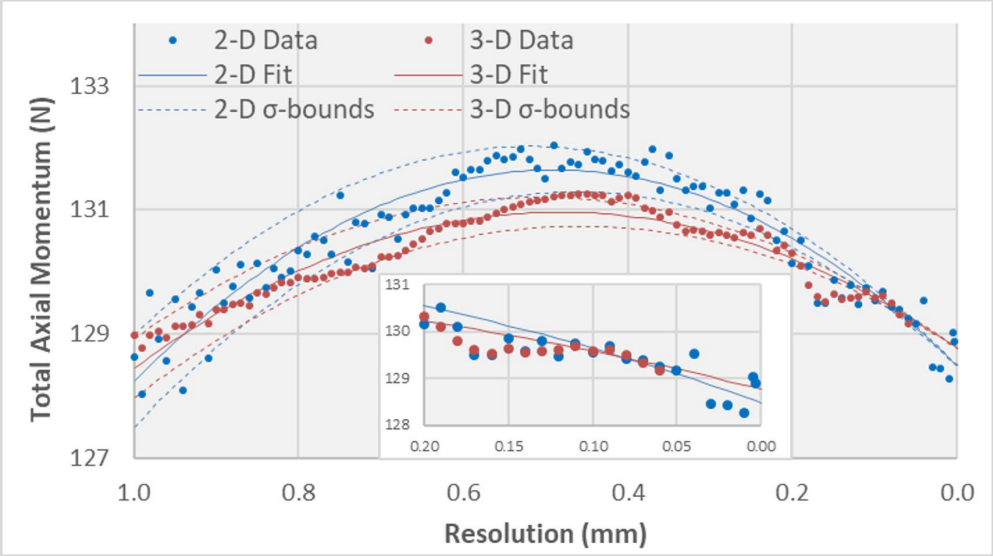

Fig. 14 Total axial momentum vs. resolution at 40 μs

6. Conclusion

This study concludes an exploration of the contribution computational factors make to uncertainty in the outcomes of numerical simulations of types commonly encountered in research of protection technologies. The influence of resolution on outcome variability was investigated in CTH simulations of SCJ formation. The structure and material states of the jet changed in a relatively continuous manner as resolution becomes finer. Expected mean values and estimated distribution widths for several jet properties as a function of resolution in 2-D and 3-D simulations were provided. As demonstrated in prior ALEGRA simulations, the temperature profile of the jet is strongly tied to the thermodynamic state at the pressure center, with jets becoming significantly hotter at coarser resolution.

7. References

1. Hornbaker DJ. Quantifying uncertainty from computational factors in simulations of a model ballistic system. Army Research Laboratory (US); 2017 Aug. Report No.: ARL-TR-8074.

2. Hornbaker DJ. Quantifying uncertainty from computational factors in simulations of a shaped charge jet. Army Research Laboratory (US); 2019 Jan. Report No.: ARL-TR-8618.

3. Hornbaker DJ. Resolution as a computational factor in ALEGRA simulations of a shaped-charge jet. Army Research Laboratory (US); 2020 May. Report No.: ARL-TR-8954.

4. Hornbaker DJ. Resolution as a computational factor in ALEGRA simulations of a shaped charge jet: supplemental study. Army Research Laboratory (US); 2020 Aug. Report No.: ARL-MR-1023.

5. Schraml S. Simulation of shaped-charge jet formation and penetration using ALE3D. Army Research Laboratory (US); 2016 Aug. Report No.: ARL-TR-7744.

6. Wong MK. CTH user's manual: CTH development project. Sandia National Laboratories; 2020 Aug 25.

7. Wong MK. Spymaster user's guide: released with CTH 12.2. Sandia National Laboratories; 2020 Aug 4.

8. Schoof LA, Yarberry VR. EXODUS II: a finite element data model. Sandia National Laboratories; 1995 Nov. Report No.: SAND92-2137.

9. Slurm workload manager. SchedMD; n.d. [accessed 2023 Sep 1]. https://slurm.schedmd.com/.

10. ParaView Developers. ParaView users guide documentation: release 5.11.0; c2020 [accessed 2023 Sep 1]. https://docs.paraview.org/en/v5.11.0/.

List of Symbols, Abbreviations, and Acronyms

2-D	two-dimensional
3-D	three-dimensional
ARL	Army Research Laboratory
DEVCOM	US Army Combat Capabilities Development Command
DoD	Department of Defense
DoP	depth of penetration
DSRC	Department of Defense Supercomputing Resource Center
HPCMP	High Performance Computing Modernization Program
SCJ	shaped-charge jet

1 (PDF)	DEFENSE TECHNICAL INFORMATION CTR DTIC OCA
1 (PDF)	DEVCOM ARL FCDD RLB CI TECH LIB
1 (PDF)	DEVCOM ARL FCDD RLA TE D HORNBAKER